

Finite Sample L_2 Bounds for Sequential Monte Carlo and Adaptive Path Selection

Joseph Marion and Scott C. Schmidler
Department of Statistical Science
Duke University

May 23, 2022

Abstract

We prove a bound on the finite sample error of sequential Monte Carlo (SMC) on static spaces using the L_2 distance between interpolating distributions and the mixing times of Markov kernels. This result is unique in that it is the first finite sample convergence result for SMC that does not require an upper bound on the importance weights. Using this bound we show that careful selection of the interpolating distributions can lead to substantial improvements in the computational complexity of the algorithm. This result also justifies the adaptive selection of SMC distributions using the relative effective sample size commonly used in the literature and we establish conditions guaranteeing the approximation accuracy of the adaptive SMC approach. We then demonstrate empirically that this procedure provides nearly-optimal sequences of distributions in an automatic fashion for realistic examples.

1 Introduction

Sequential Monte Carlo (SMC) is a sampling method that moves particles drawn from an initial distribution μ_0 to a target distribution π via a sequence of interpolating distributions $\mu_0, \dots, \mu_S = \pi$. Choosing an appropriate sequence of distributions, which we refer to as a *path* [1, 2], is critical to obtaining an efficient SMC sampler. Common path selection approaches for static (fixed dimension) SMC problems include batch processing with data [3], tempering with deterministic schedules [4–6], and tempering with adaptively chosen temperatures [2, 6, 7]. Comparison of paths is generally limited to simulation studies; the theoretical SMC literature treats the sequence of interpolating distributions as given and does not consider the effect of path selection on the accuracy of the resulting SMC estimator [8–13].

In the first part of this paper, we directly relate the computational complexity of obtaining a bounded-error SMC estimator to the selection of interpolating distributions. More formally, we demonstrate conditions under which SMC provides a *randomized approximation scheme* for estimating expectations of π . The bound presented here improves on the recent results in [14], relaxing the assumption of bounded density ratios and requiring only a bound on the L_2 distance between adjacent distributions. This allows us to explicitly relate the distributions in the selected path to the error in the resulting estimator and the

computational complexity of the algorithm. This in turn allows us to identify sequences of interpolating distributions (paths) that lead to substantial improvements in efficiency. Unlike other finite sample results for SMC in the literature [8, 9, 14], it also enables us to establish the convergence of SMC in situations where the importance sampling weights are unbounded.

We use this new bound to illustrate the improvements obtainable by better path selection on two examples. The first is a spherical Gaussian target distribution, where we show that a path using geometric mixtures and tempering has superior complexity to a path using only geometric mixtures. The second example considers general log-concave target distributions. We use the path from [15] in combination with the sampling algorithm from [16] to provide an upper bound for SMC that obtains state of the art complexity for this problem.

In practice, pre-specifying a sequence of distributions that efficiently controls the L_2 distance between steps may be difficult. The second part of the paper provides a practical scheme for adaptively choosing a sequence of distributions so that the L_2 distance between steps is provably controlled when weights are bounded. This is accomplished through monitoring the relative effective sample size (RESS). Adaptive path selection using the RESS is well known to the SMC community [2, 6, 7]; we provide conditions under which the RESS can be used to estimate the L_2 distance between steps with high accuracy, justifying its use for choosing an SMC path. We then extend our error bounds to this adaptive situation, giving conditions under which SMC using adaptive path selection remains a randomized approximation scheme.

We conclude by demonstrating that this algorithm has good empirical performance on two examples. The first is a mean field Ising model, where we show that the adaptive SMC using tempered distributions finds nearly optimal sequences of interpolating distributions. The second is a Bayesian linear regression using a data-tempering approach. We demonstrate that the traditional path may result in steps with large L_2 distances causing significant instability in the resulting estimator. This problem is addressed using a hybrid path that combines the computational advantages of data-tempering with the stability of traditional tempering and provides bounded errors.

2 SMC error bounds

Before stating the main result we introduce some notation and describe the SMC algorithm studied in this paper. Let $(\mathcal{X}, \mathcal{B}, \lambda)$ be a probability space. Define \mathcal{P} be the set of probability measures on \mathcal{X} that are absolutely continuous with respect to λ and \mathcal{F} the set of measurable functions $f : \mathcal{X} \rightarrow \mathcal{R}$. Each measure acts on functions $f \in \mathcal{F}$ from the left by $\mu f = \int f(x)\mu(dx) = \mathbf{E}f$. We say that a measure $\nu \in \mathcal{P}$ is ω -warm with respect to μ if $\sup_{B \in \mathcal{B}(\mathcal{X})} \nu(B) \leq \omega \cdot \mu(B)$ [17, 18]. Let $\mathcal{P}_\omega(\mu)$ be the set of all such measures. For an ergodic Markov kernel $K : \mathcal{X} \times \mathcal{B} \rightarrow [0, 1]$ with limiting distribution μ , define the ω -warm mixing time of K by $\tau_K(\epsilon, \omega) = \min \{t : \sup_{\nu \in \mathcal{P}_\omega(\mu)} \|\nu K^t - \mu\|_{\text{TV}} \leq \epsilon\}$, where $\|\cdot\|_{\text{TV}}$ denotes the total variation distance.

In this paper we study the following SMC algorithm. Before sampling, the user specifies a path μ_0, \dots, μ_S where $\mu_s \in \mathcal{P}$ and $\mu_{s-1} \ll \mu_s$. We abuse notation and write the density $\mu_s(x) = q_s(x)/z_s$ where $q_s(x)$ is a known, unnormalized density. The algorithm is initialized by drawing N samples $X_0^{1:N} = X_0^1, \dots, X_0^N$ independently from μ_0 , then proceeds in S steps. At the beginning of step s , each particle is assigned an importance sampling weight $w_s(X_{s-1}^n) = q_s(X_{s-1}^n)/q_{s-1}(X_{s-1}^n)$. Then, a new set of particles $\tilde{X}_s^{1:N}$ is

drawn with replacement from the current particles according to the weights (multinomial resampling); i.e. a copy of X_{s-1}^n is drawn with probability proportional to $w_s(X_{s-1}^n)$. Finally, each resampled particle evolves independently according to a Markov kernel K_s with stationary distribution μ_s , resulting in a new set of particles $X_s^n \sim K^t(\tilde{X}_s^n, \cdot)$. Following step S of the algorithm πf is estimated using the particle average $\hat{\pi} f = \frac{1}{N} \sum_{n=1}^N f(X_S^n)$. Detailed descriptions of this SMC algorithm can be found in [3, 4, 14].

2.1 Convergence of SMC using the L_2 distance

The convergence result presented in this section depends on the L_2 distance between interpolating distributions and the mixing times of the Markov kernels. For $\mu, \eta \in \mathcal{P}$ define the L_2 distance from η to μ by the $L_2(\mu)$ norm of η/μ :

$$\|\eta/\mu\|_{L_2(\mu)} = \int \left(\frac{\eta(dx)}{\mu(dx)} \right)^2 \mu(dx)$$

This quantity is not symmetric and therefore not a true metric, however we follow standard convention and refer to it as the L_2 distance because it provides an appropriate measure of the divergence between μ and η . Note that subtracting one yields the traditional χ^2 “distance” which plays a familiar role in importance sampling, where it provides the variance of the importance weights under instrumental distribution μ and target distribution η . This idea has been used in SMC, where the empirical variance of the weights is used to assess the efficiency of the particle system at each step, using the relative effective sample size (RESS):

$$\hat{E}_s = \frac{\left(N^{-1} \sum_{s=1}^N w_s(X_{s-1}^n) \right)^2}{N^{-1} \sum_{s=1}^N w_s(X_{s-1}^n)^2} \quad (1)$$

When \hat{E}_s is small the particle system is described as degenerate. As $n \rightarrow \infty$, \hat{E}_s converges to $\mathcal{E}_s \triangleq \|\mu_s/\mu_{s-1}\|_{L_2(\mu_{s-1})}^{-1}$, the reciprocal of the L_2 distance; we therefore interpret the RESS as an estimate of \mathcal{E}_s and in Section 4 give bounds on its approximation error. Our main result bounds the approximation error of SMC in terms of a bound on the maximal L_2 distance between adjacent distributions:

$$\|\mu_s/\mu_{s-1}\|_{L_2(\mu_{s-1})} \leq \mathcal{E}^{-1} \quad (2)$$

Theorem 1 establishes conditions under which SMC serves as a *randomized approximation scheme*. An algorithm is a randomized approximation scheme if, for any user-specified $\epsilon > 0$ and $\delta \in (0, 1]$, it guarantees $|\hat{\pi} f - \pi f| < \epsilon$ with probability at least $1 - \delta$ [19]. To simplify the presentation, we establish this for $\delta = 1/4$, but this is easily improved to arbitrary $\delta > 0$ at a cost of $\mathcal{O}(\log(1/\delta))$ using the median approach [20].

Theorem 1 (Error bound for SMC).

Fix $\epsilon > 0$ and sample $X_0^{1:N}$ independently from μ_0 . Let $\|\mu_s/\mu_{s-1}\|_{L_2(\mu_{s-1})} \leq \mathcal{E}^{-1} < \infty$. Choose

1. $N \geq 2 \log(16S) \cdot \max\left\{\frac{42}{\epsilon}, \frac{1}{\epsilon^2}\right\}$
2. $t \geq \max_s \tau_s\left(\frac{1}{8NS}, 2\right)$

Then for any $f \in \mathcal{F}$ with $|f| \leq 1$,

$$|\hat{\pi} f - \pi f| \leq \epsilon.$$

with probability at least $3/4$.

The proof of Theorem 1 is given in the appendix and closely follows the proof of Theorem 1 in [14]. The key difference is the use of an improved martingale concentration inequality to ensure concentration of the weights, which replaces Lemma 4 of [14] and results in a modified one-step induction condition yielding Theorem 1 above.

Assumption (2) replaces the upper bound W on the weights and a lower bound Z on the ratios of normalizing constants required by [14]. When such bounds are available we immediately have $1/\mathcal{E} \leq W^2 Z^2$ to apply Theorem 1. However, requiring a bound on $\frac{1}{\mathcal{E}}$ instead has several advantages. First, the assumption of bounded weights restricts the sequences of interpolating distributions that can be considered and is frequently violated in applications. (Despite this, it is commonly assumed in theoretical results for both asymptotic and finite sample convergence of SMC). Another advantage of assumption (2) is that we can compare the resulting SMC bounds directly to similar bounds for MCMC. This advantage is explored in the next section.

3 Path selection and complexity

Finite sample bounds such as Theorem 1 facilitate explicit comparison between algorithms. In this section, we compare our bounds on the computational complexity of SMC with existing bounds for MCMC to highlight the advantages of each algorithm. Complexity is given in total number of Markov kernel transitions required to approximate πf . Suppose that K_1, \dots, K_S are geometrically ergodic and reversible with spectral gaps $\rho_1, \dots, \rho_S \in (0, 1)$. Then the number of transitions according to K_S required to sample approximately from π using a Markov chain starting with a draw from μ_0 is [21, 22]

$$\mathcal{O}\left(\frac{\log \|\mu_0/\pi\|_{L_2(\pi)}}{\rho_S}\right)$$

In comparison, Theorem (1) gives the following complexity bound for SMC

$$\mathcal{O}\left(\frac{S/\mathcal{E} \cdot \log^2(S/\mathcal{E})}{\rho^*}\right)$$

where $\rho^* = \max_s \rho_s$. When the spectral gaps of the Markov kernels K_s are of the same order, the bounds differ primarily by the cost of moving from the initial distribution to the target distribution. For MCMC, this factor is $\log \|\mu_0/\pi\|_{L_2(\pi)}$, whereas for SMC this factor is an upper bound on $S/\mathcal{E} \geq S \cdot \max_s \|\mu_s/\mu_{s-1}\|_{L_2(\mu_{s-1})}$, which we call *the path length*. Note that the L_2 distance is not symmetric and the SMC and MCMC bounds depend on this quantity in opposite directions, and therefore differ even for $S = 1$ (importance sampling). For example when μ_0 is heavy tailed relative to π , $\|\mu_0/\pi\|_{L_2(\pi)}$ may be much larger than $1/\mathcal{E}$. Since specifying the initial distribution μ_0 to be heavier tailed than the target π is generally easier than the reverse, this indicates an advantage for SMC. On the other hand, the amount of computation required by SMC grows linearly in S/\mathcal{E} whereas the bound for MCMC grows logarithmically in $\|\mu_0/\pi\|_{L_2(\pi)}$. This can be advantageous for MCMC when finding a sequence of distributions that ensures S/\mathcal{E} small is difficult.

The remainder of this section compares the relative cost of moving from μ_0 to π for SMC versus MCMC. The first example investigates the problem of sampling from a spherical Gaussian target distribution, studying the path complexity with regards to the target precision, mean, and dimension. The second example considers the problem of sampling a general log-concave target distribution and uses an optimal

path identified by [15] to obtain an SMC path with low complexity. This bound improves upon the best existing results for MCMC.

3.1 Gaussian example

Consider the problem of approximating expectations with respect to a d -dimensional spherical Gaussian target distribution $\pi(x) = N_d(1_d \cdot \theta, I_d/\phi)$, where $\theta \geq 2$ and $\phi \geq 1$. This problem is representative of many Bayesian inference problems with large sample sizes via the Bernstein-von Mises theorem. A simpler version of this problem (with $\theta = 0$) was studied by [14]; however, results for the more challenging problem when $\theta \neq 0$ are now possible as Theorem 1 allows for unbounded importance sampling weights.

We assume that the initial distributions for both SMC and MCMC are chosen to be standard Gaussian, $\mu_0 = N_d(0, I_d)$. The cost of MCMC, relative to the spectral gap, is given by

$$\mathcal{O}\left(\frac{\theta^2 d}{\phi(2-\phi)}\right) \quad (3)$$

assuming $\phi < 2$ (see Appendix). We will consider two different choices of the interpolating distribution sequences for SMC which lead to bounds with improved complexity with respect to ϕ , θ and d . These results are applicable for any $\phi \geq 1$.

A standard approach to constructing a sequence of interpolating distributions is a geometric path, with $\mu_\beta(x) \propto \mu_0(x)^{1-\beta} \pi(x)^\beta$ for $\beta \in [0, 1]$. Such paths are commonly used to estimate ratios of normalizing constants, where they are sometimes referred to as power paths or tempered paths [1, 23]. The path is specified by a sequence $\beta_0 = 0 \leq \beta_1 \leq \dots \leq \beta_S = 1$ controlling the rate at which the path moves from μ_0 to π . Choosing $\beta_s = (1 + \frac{2}{\theta\sqrt{d}})^{s-1} / (\phi \cdot \theta\sqrt{d}) \wedge 1$ and $S = 1 + \lceil \frac{\theta\sqrt{d}}{2} \log(\phi^2 \cdot \theta\sqrt{d}) \rceil$ ensures $\|\mu_s/\mu_{s-1}\|_{L_2(\mu_{s-1})} \leq \mathcal{O}(1)$ and gives an upper bound on path length S/\mathcal{E} of (see Appendix A.2):

$$\mathcal{O}\left(\theta\sqrt{d} \cdot \log(\phi^2 \cdot \theta\sqrt{d})\right) \quad (4)$$

This bound displays an improvement in dimension dependence from $\mathcal{O}(d)$ to $\mathcal{O}(\sqrt{d} \log \sqrt{d})$ relative to the MCMC bound. We also see a super-exponential improvement in dependence on the precision, from $\mathcal{O}(\frac{1}{\phi-2})$ to $\mathcal{O}(\log \phi)$, as well as an improvement in the location dependence from $\mathcal{O}(\theta^2)$ to $\mathcal{O}(\theta \log \theta)$.

However there exists an even better path inspired by a result from [1]. First, choose $s_1 = \lceil 3\sqrt{d} \log(d\theta^2) \rceil$ distributions to be $\mu_s = N_d(0, I_d/\phi_{1,s})$ with $\phi_{1,s} = (1 - 1/\sqrt{9d})^s \vee \frac{1}{d\theta^2}$. The next distribution changes the location in a single step: $\mu_{s_1+1} = N_d(1_d\theta, I_d \cdot d\theta^2)$. Finally, we take $s_2 = \lceil \sqrt{d} \log(d\theta^2\phi) \rceil$ steps using $\mu_s = N_d(1_d\theta, I_d/\phi_{2,s})$ with $\phi_{2,s} = \frac{1}{d\theta^2} \left(1 + 1/\sqrt{d}\right)^{s-s_1-1} \wedge \phi$. We call this the *precision path* because it uses the fact that when the precision is sufficiently small it is possible to move between normal distributions with differing locations in a single step. Because precision can be decreased exponentially quickly, this shortens the overall path, yielding an improved complexity in θ compared to varying the mean and precision simultaneously. More precisely, the precision path ensures $1/\mathcal{E} \leq 2$, giving a path length bound of (see Appendix A.3):

$$\mathcal{O}(\sqrt{d} \log(\phi \cdot \theta^2 d)) \quad (5)$$

showing an improvement from $\mathcal{O}(\theta \log \theta)$ to $\mathcal{O}(\log \theta)$. This example highlights the potential speedup available using non-geometric paths, though finding such paths may be challenging.

Gelman and Meng [1] derived an optimal path sampling estimator to estimate (log-) ratios of normalizing constants between normal distributions with different means. This optimal path also flattens the intermediate normal distributions by reducing their precisions, resulting in a similar improvement in complexity from $\mathcal{O}(\theta)$ (tempered path) to $\mathcal{O}(\log \theta)$. The similarity between good path-sampling and SMC paths arises due to the necessity of estimating intermediate ratios of normalizing constants to satisfy the one-step induction condition for SMC shown in [14]. In fact, when $d = 1$ and $\phi = 1$, a sufficiently fine discretization of the Gelman and Meng path yields the same complexity bound as the precision path. It is unlikely that this path is optimal for SMC, however, since the optimal path-sampling sequence from π to μ_0 is the reverse of the optimal path from π to μ_0 , while this will not generally be true for SMC as the L_2 "distance" is asymmetric and optimal paths should reflect this asymmetry.

3.2 Log-concave target distributions

Let $\pi(x) \propto q(x)$ be a log-concave target distribution on \mathcal{R}^d . A function q is said to be strongly log-concave if $q^{1-\alpha}(x) \cdot q^\alpha(y) < q(\alpha x + (1-\alpha)y)$ for $x, y \in \mathcal{R}^d$ and $\alpha \in (0, 1)$. In general bounds on the ω -warm mixing times of Markov kernels targeting a sequence of distributions obtained by tempering a log-concave distribution will have the same complexity at each step. For example, if we choose K_s to be the Metropolis-adjusted Langevin algorithm (MALA) [24], the complexity of the bound on the ω -warm mixing time is independent of the temperature parameter [14, 16] and a similar result holds for other Markov kernels including the *ball-walk* or *hit-and-run walk* Markov kernels [25]. Therefore, when the target distribution is log-concave, we can again focus on finding interpolating sequences that minimize the path length.

Efficient path selection for log-concave distributions has received substantial attention in the theoretical computer science literature, where the volume of a convex body is estimated by sampling from a sequence of tempered distributions [15, 26]. A key factor in volume computation is the L_2 distance between adjacent distributions, which controls the relative error when estimating the corresponding volume ratios. The following corollary follows from Theorem 1, using the the tempering path from [15] and the bounds on the mixing time from [16].

Corollary 1.1 (SMC complexity for log-concave target distributions). *Let $\pi(x) \propto q(x)$ be log-concave with mode x^* and define $\kappa = L/m$ where for all $x, y \in \mathcal{R}^d$:*

$$-\frac{L}{2} \|x - y\|_2^2 \leq \log \frac{q(x)}{q(y)} - \nabla \log q(x)^T (x - y) \leq -\frac{m}{2} \|x - y\|_2^2$$

Restrict π to the ball B of radius $4\sqrt{d/m}$ centered at x^ and assume $\epsilon > 2e^{-d}$. Choose $\mu_0 \propto \mathbb{1}_B(x)$ and $\mu_s(x) \propto \pi^{\beta_s}(x) \mathbb{1}_B(x)$ with $\beta_s = \frac{1}{d\kappa} \left(1 + \frac{1}{\sqrt{d}}\right)^s$ for $s = 1, \dots, S = \lceil \sqrt{d} \log(d\kappa) \rceil$. Let K_s be a MALA kernel with step size given in [16]. Then SMC provides a randomized approximation scheme in time:*

$$\mathcal{O}^* \left(d^{3/2} \kappa \cdot \max \{1, \sqrt{\kappa/d}\} \right)$$

The notation \mathcal{O}^* indicates the omission of logarithmic terms in d and κ . The specified path ensures $1/\mathcal{E} \leq \epsilon$ and gives $S/\mathcal{E} = \mathcal{O}(\sqrt{d} \log(d\kappa))$ [15]. The MALA kernel provides an ω -warm mixing time of $\mathcal{O}\left(d\kappa \cdot \log \frac{2\omega}{\epsilon} \cdot \max \{1, \sqrt{\kappa/d}\}\right)$ [16], and the result then follows from Theorem 1. The restriction to B is used to bound the L_2 distance of the first step and has minimal impact on the results of our analysis as

$\pi(B) \geq 1 - \epsilon/2$; similar restrictions are common in the log-concave sampling literature. The assumption $\epsilon > 2e^{-d}$ serves only to simplify the presentation.

The result in Corollary 1.1 improves on the $\mathcal{O}^*(d^k \kappa^2 \cdot \max\{1, \sqrt{\kappa/d}\})$ result in [14] and the state-of-the-art bound for MCMC of $\mathcal{O}^*(d^2 \kappa \cdot \max\{1, \sqrt{\kappa/d}\})$ [16]. In both cases, the improvement comes solely from the selection of a superior path, as each bound uses the same Markov kernels. To the best of our knowledge, this is the fastest randomized approximation scheme for a log-concave target distribution. We remark, however, that an ever better bound could be obtained by combining the path in [15] with the MALA mixing times in [16] using a time-inhomogenous Markov chain.

4 Adaptive path selection

Selecting a path where a bound on the L_2 distance is known *a priori*, let alone an optimal path, can be difficult in practice. In this section we establish conditions under which adaptively choosing distributions using the RESS, as commonly done in practice [2, 6, 7], automatically selects a path with controlled L_2 distance between steps. Given a pre-specified bound $\mathcal{E} \in (0, 1)$, suppose μ_s is chosen from a (possibly large) discrete set of candidate distributions $\nu_{s,1}, \dots, \nu_{s,M} \in \mathcal{P}$. (For example, this would be the case in adaptive tempering when considering temperature changes of increasing size.) For each candidate distribution, we compute the RESS $\hat{E}_{s,m}$ and choose $\mu_s \in \{\nu_{s,m}\}$ so that $\hat{E}_{s,m} \geq \mathcal{E}$. We give conditions under which $\frac{1}{\hat{E}_{s,m}}$ accurately estimates $\|\eta_{s,m}/\mu_{s-1}\|_{L_2(\mu_{s-1})}$ and so μ_s can be chosen so that $\|\mu_s/\mu_{s-1}\|_{L_2(\mu_{s-1})} \leq 3/\mathcal{E}$ with high probability. We then apply the same techniques used to prove Theorem 1, ensuring that the chosen step will preserve the approximation accuracy of the algorithm with high probability. The section begins by discussing the specification and selection of candidate distributions. Then, we extend the results of Theorem 1 to the adaptive setting, giving conditions under which the adaptive algorithm constitutes a randomized approximation scheme.

4.1 Candidate distributions

At step s of the algorithm, we choose μ_s from a finite set of candidate distributions $\nu_{s,1}, \dots, \nu_{s,M}$. This set may depend on μ_{s-1} but not on the particle values themselves. We assume these candidates are ordered *a priori*, such that a move to $\nu_{s,m}$ is preferred over a move to $\nu_{s,m-1}$. The algorithm proceeds by computing the RESS of the particle system under each candidate distribution:

$$\hat{E}_{s,m} = \frac{\left(N^{-1} \sum_{s=1}^N w_{s,m}(X_{s-1}^n)\right)^2}{N^{-1} \sum_{s=1}^N w_{s,m}(X_{s-1}^n)^2} \quad (6)$$

where $w_{s,m}(x) \propto \frac{\nu_{s,m}(x)}{\mu_{s-1}(x)}$. In order to obtain bounds for the adaptive algorithm, we require the set of candidate distributions to have bounded weights; i.e. $0 < w_{s,m} \leq 1$ for each s and m . This differs from the setting of Theorem (1). The next distribution is chosen to be the candidate distribution with sufficiently large RESS that is closest to π :

$$\mu_s = \max_m \left\{ \nu_{s,m} : \hat{E}_{s,m} \geq \mathcal{E} \right\} \quad (7)$$

When \mathcal{E} is close to 1 the SMC algorithm will take small steps, preserving particle approximations with high effective sample sizes. On the other hand, when \mathcal{E} is close to 0, the algorithm will take larger steps leading to particle approximations where it is possible for relatively few particles to receive substantial weight.

Example: geometric path. Let μ_0 be an initial distribution on \mathcal{X} and define $\mu(x | \beta) \propto \mu_0(x)^{1-\beta} \cdot \pi(x)^\beta$ for $\beta \in [0, 1]$ to be the geometric mixture of μ_0 and π . At step s of the algorithm, the previous distribution is $\mu_{s-1} = \mu(x | \beta_{s-1})$ and the candidate distributions are $\nu_{s,m}(x) = \mu(x | \beta_{s,m})$ with $\beta_{s,m} = \beta_{s-1} + \frac{m}{M}(1 - \beta_{s-1})$.

Computing the weights for each candidate distribution is greatly simplified by pre-computing $w^n \propto \pi(X_{s-1}^n) / \mu_0(X_{s-1}^n)$ as $w_{s,m}(X_{s-1}^n) = (w^n)^{\beta_{s,m}}$. The optimal candidate distribution can then be found in $\mathcal{O}(\log M)$ time using binary search and is unique as $1/\hat{E}_{s,m}$ is non-increasing with m .

Example: data tempered path. Let $\pi(x) \propto p(y_{1:K}|x)\pi_0(x)$ be a posterior distribution arising from a Bayesian model with K observations and prior distribution π_0 . An alternative to the power path is a sequential posterior obtained by adding observations to the likelihood [3]. Let $\mu_{s-1}(x) \propto p(y_{1:k_{s-1}}|x)\pi_0(x)$ where $y_{1:k_s}$ denotes the first $0 < k_s < K$ observations. The candidate distributions are chosen from $\nu_{s,m}(x) \propto p(y_{1:k_{s,m}}|x)\pi_0(x)$ for $k_{s-1} < k_{s,1} < \dots < k_{s,M} \leq K$.

When the likelihood is independent, i.e. $p(y_{1:K}|x) = \prod_{k=1}^K p(y_k|x)$, the weights can be computed incrementally as $w_{s,m}(X_{s-1}^n) = w_{s,m-1}(X_{s-1}^n) \cdot \prod_{k=1+k_{s,m-1}}^{k_{s,m}} p(y_k|X_{s-1}^n)$. Rather than choosing the largest m to satisfy condition (7) it is generally expedient find the first m such that this condition fails and choose $\mu_s = \nu_{s,m-1}$.

Data tempering may be preferred to tempering in practice as it can substantially reduce the number of likelihood evaluations needed to approximate a posterior distribution while also providing a tempering effect. A drawback of this approach is that the set of candidate distributions may not be sufficiently fine, making it impossible to select a distribution satisfying (7). In Section 5.2 we introduce a hybrid path, which combines the advantages of both the geometric and data-tempering paths.

4.2 An adaptive path selection RAS

To obtain conditions under which the adaptive step size SMC algorithm provides an RAS, we present a slightly modified version the algorithm. Begin by fixing an initial number of steps S , samples N_1 , Markov kernel transitions t_1 , and a target RESS \mathcal{E} . Select distributions according to the following adjusted criteria:

$$\mu_s = \max_m \left\{ \nu_{s,m} : \hat{E}_{s,m} \geq \mathcal{E} \text{ and } \bar{w}_{s,m}^2 \geq C \right\} \quad (8)$$

The additional requirement that $\bar{w}_{s,m}^2 \geq C$ for pre-specified $C \in (0, 1)$ is used to ensure that $1/\hat{E}_{s,m}$ approximates $\|\nu_{s,m}/\mu_{s-1}\|_{L_2(\mu_{s-1})}$ with bounded relative error. Small values of C may allow for bigger steps, however, this advantage must be balanced by against the number of particles required which will increase as $\mathcal{O}(C^{-2})$.

To establish adaptive step size SMC as an RAS we requires an additional modification of the algorithm, as the proof of Theorem 1 requires that N depend on the number of steps S , which is not known in advance for the adaptive algorithm. To achieve a randomized approximation, the number of particles must be

allowed to grow as the number of steps adaptively increases. This can be done in a straightforward way, by choosing N based on S and then increasing N if π is not reached within the first S steps. To increase N , N' new samples are drawn independently from μ_0 , evolved through the previously chosen path μ_1, \dots, μ_S , and used to supplement the existing particles yielding a system of size $N' + N$. A natural choice is doubling ($N' = N$), ensuring that the particle system is valid for S additional steps before doubling is required again. We call these repetitions *epochs*, and denote the current epoch by p . The number of Markov kernel transitions must also be increased at each epoch as this also depends on the N and S .

A disadvantage of the doubling approach is that the total number of particles at the end of epoch p is $2^p N$. This exponential dependence can be reduced to sub-quadratic by following a procedure that chooses the number of additional particles at each epoch more carefully. This procedure is summarized in algorithm 1

Algorithm 1: Adaptive SMC algorithm

Result: $\Pr(|\hat{\pi}f - \pi f| \leq \epsilon) \geq 3/4$ for any $f \in \mathcal{F}$ with $|f| \leq 1$

Fix $\mathcal{E} \in (0, 1)$ and $S > 0$;

Set $p = 0, s = 0, t = 0$;

while $\mu_s \neq \pi$ **do**

$s = s + 1$;

if $s = p \cdot S$ **then**

Set $p = p + 1$ and $t = t_p$;

Apply SMC to N_p new particles using the path $\mu_0, \dots, \mu_{S(p-1)}$;

Add the new particles to the set of current particles;

end

Select μ_s from $\eta_{s,1}, \dots, \eta_{s,M}$ according to (8);

Apply a step of SMC targeting μ_s ;

end

Under the following conditions this adaptive SMC algorithm provides a randomized approximation scheme

Theorem 2 (Error bound for adaptive SMC).

Choose a set of paths according to Section 4.1 with $0 < w_{s,m} \leq 1$ for each candidate distribution. Fix an error tolerance $\epsilon > 0$, a target RESS $0 < \mathcal{E} < 1$, an epoch length S , and a lower bound $0 < C < 1$. Let:

1. $N_1 \geq \max \left\{ \frac{32}{C^2} \log(96SM), \frac{243}{\mathcal{E}} \log(24S), \frac{2}{\epsilon^2} \log(24S) \right\}$
2. $N_p \geq \max \left\{ \frac{243(\log(24S)+p)}{\mathcal{E}}, \frac{23}{C^2}, \frac{2}{\epsilon^2} \right\}$
3. $t_e \geq \sup_{s,m} \tau_{\nu_{s,m}} \left(\frac{1}{2^{p-1} \max \{ N_p \cdot S^p, \sum_{i=1}^p N_i \}}, 2 \right)$

Then for any $f \in \mathcal{F}$ with $|f| \leq 1$ Algorithm 1 ensures

$$|\hat{\pi}f - \pi f| \leq \epsilon.$$

with probability at least 3/4.

Proof of Theorem 2 is given in the appendix. At the end of epoch p , the total number of particles is $\mathcal{O}(p \cdot \max\{\frac{\log(24S+p)}{\varepsilon}, C^{-2}, \epsilon^{-2}\})$, a substantial improvement on the exponential dependence of the doubling algorithm. Despite the substantial improvement in p , it is still generally more efficient to choose S large so that p remains small, as the complexity of the algorithm grows only logarithmically in S . In fact, when the candidate distributions are chosen so that there is a maximum possible path length S^* , as in data tempering where $S^* = K$, it may be most efficient to choose $S = S^*$ as this ensures $p = 1$.

To our knowledge Theorem 2 provides the first proof of convergence for SMC with adaptively chosen sequences of distributions. Previously, in order to ensure that a central limit theorem held in the adaptive setting, a two stage approach to SMC was employed [6,27] in which an adaptive SMC algorithm was run to select a path, followed by a non-adaptive SMC run on the selected path to estimate expectations under π . Our result shows that for appropriately chosen N and t , this two stage procedure is unnecessary. In addition, the two stage procedure provides no information about the properties of the chosen path or the resulting estimation error. Theorem 2 may also be seen as a validation of the use of the RESS for selecting distributions. Other approaches have been considered [28,29], however, these methods currently lack theoretical support.

Note that we have given no conditions that ensure it is possible to choose an interpolating distribution satisfying (8); if this condition is not met the algorithm will terminate prematurely. We can also make no claims at this point about near-optimality of the selected path in terms of path length. We explore this issue in the next section. Finally, the additional requirement of the lower bound C in (8) may be unnecessarily restrictive in practice, but it is unclear at this time if selecting distributions according to (7) is sufficient.

5 Empirical results

We investigate the empirical performance of the adaptive step-size SMC algorithm on two non-trivial target distributions where the L_2 distance can be evaluated exactly. Our goals are twofold. First, the conditions of Theorem 2 are generally difficult to ensure due to the challenge of bounding the mixing time. Therefore, it is sensible to verify whether a naive implementation of the algorithm might maintain controlled L_2 distances at each step. Second, our result says little about the relative optimality of the adaptively chosen path, guaranteeing accurate estimation but not optimal path length. This empirical study allows us to compare adaptively chosen paths to an ideal path which maintains a fixed step size of \mathcal{E} . Finally, we provide an example where data tempering may lead to paths where condition (7) cannot be satisfied. We introduce a hybrid path that addresses this problem, ensuring condition (7) is met at each stage of the algorithm. Empirically, we find that the hybrid approach decreases the overall path length and leads to paths of near-optimal length for a specified step size. For these reasons, we recommend that the hybrid approach be used over the data tempering approach in practice.

5.1 Example: Ising model

Consider the well-known mean field Ising model originally developed as a model of ferromagnetism in statistical physics. The D -dimensional model takes values in $\mathcal{X} = \{-1, 1\}^D$ for binary ‘‘spins’’ x_d with

probability

$$\pi(x|\alpha) \propto \exp\left(\frac{\alpha}{2D}\left(\sum_{d=1}^D x_d\right)^2\right)$$

When $\alpha > 0$, the high probability configurations are those where the spins are mostly the same. The hyperparameter α controls the strength of this effect. Related models have been used in machine learning for image processing [30] and in Bayesian statistics for modeling spatial dependence [31].

Sampling from the Ising model has received considerable attention [32, 33]. A key characteristic of the model is that π undergoes a phase transition as α approaches the critical temperature α_0 . This is exhibited in the distribution of the magnetization $M = \sum_{d=1}^D x_d$, which rapidly changes from concentrated about 0 to dispersed to the extremes near $M = D$ and $M = -D$. This rapid change in behaviour makes it challenging to sample from the Ising model when $\alpha > \alpha_0$ as it is difficult for MCMC methods to move between these modes. Tempering approaches have proven successful at sampling from this distribution [34]. The selection of an appropriate temperature ladder is crucial to the success of parallel tempering, and subsequently selecting a temperature ladder has received substantial attention in the tempering literature. In contrast, we demonstrate empirically that temperature selection using an adaptive SMC approach achieves nearly optimal performance in the sense of minimizing the number of steps (temperatures) for a given \mathcal{E} .

For $D \in \{10, 50, 250\}$ and $\alpha = 2 \geq \alpha_0$ we performed SMC using the geometric path given in Section 4.1 with μ_0 uniform distribution on \mathcal{X} . Markov transitions are made according to the Glauber dynamics (Gibbs sampling), scanning through each component in a randomly chosen order and drawing a new spin from its conditional distribution. We set $\mathcal{E} = 0.5$ and used 1,000 particles for each simulation. This SMC procedure was repeated 1,000 times to assess variability. We then computed the error of the estimated L_2 distance at each step relative to the exact L_2 distance, which can be evaluated numerically. We also compared the adaptively chosen path to the temperature ladder satisfying $\|\mu_s/\mu_{s-1}\|_{L_2(\mu_{s-1})} = 2$ at each step.

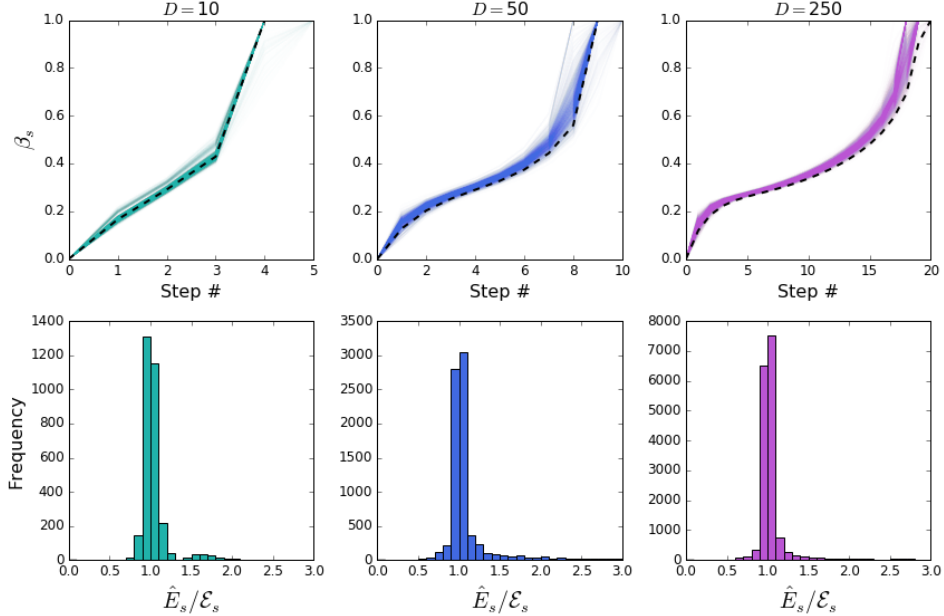


Figure 1: Results of the empirical path selection for the mean field Ising model. The top row shows the distribution of paths chosen by the adaptive approach, with the optimal path given by the dotted black line. The bottom row shows the distribution of the estimated L_2 distances relative to the true distance.

The results of the experiment are displayed in Figure 1. In general, the adaptively chosen paths follow closely the optimal path, being of comparable length and displaying similar curvature near the critical temperature where they take small steps as the target distribution is changing rapidly. Estimated values of $\|\mu_s/\mu_{s-1}\|_{L_2(\mu_{s-1})}$ are generally quite accurate. More importantly, the induction condition prescribed by Lemma 4 is achieved at each step of the algorithm and across every step of the simulation. The selection criteria in (7) is sufficient to achieve good path selection for this problem, perhaps not requiring the modified criteria (8).

5.2 Bayesian linear regression

Our second example demonstrates the behaviour of adaptive SMC using data tempering. Consider a Bayesian linear regression model with $Y = X\beta + \epsilon$, where $Y \in \mathcal{R}^K$ is a response vector, $X \in \mathcal{R}^{K \times D}$ is a matrix of covariates, $\beta \in \mathcal{R}^D$ is an unknown coefficient vector and $\epsilon \sim N(0, I_K \cdot \sigma^2)$ is a vector of observation noise. We fit the white wines data set from the UCI machine learning repository [35], which consists of $M = 4898$ observations of wine quality and $D = 11$ physicochemical predictors. Before analysis, the data was centered and scaled. We adopt a normal inverse-gamma prior with $\pi_0(\beta | \sigma^2) \propto N(0, \sigma^2(X^T X)^{-1}/K)$ and $\pi_0(\sigma^2) \sim \text{Inv-Gamma}(4, 4)$. This prior is conjugate, allowing analytic calculation of the L_2 distance between SMC steps for comparison (see appendix C).

We simulated from the posterior distribution of this model using the data tempering approach described in Section 4.1. During the initial phase of the algorithm, the target distribution changes rapidly as observations are added, making it difficult to obtain transitions with sufficiently high relative effective sample size. As a result, instead of choosing $\mu_0 = \pi_0$, we let $\mu_0 \propto p(Y_{1:200} | \beta, \sigma^2, X_{1:200}) \cdot \pi_0(\beta, \sigma^2)$.

This starting point can be easily obtained in practice, either by MCMC or via a geometric path from the prior distribution. The Markov kernels are chosen to be Gibbs samplers, alternating draws of $\beta \mid \sigma^2$ and $\sigma^2 \mid \beta$. We conducted 1,000 SMC runs, each adaptively choosing a path with $\mathcal{E} = 1/2$. Observation ordering was permuted randomly between each trial to assess the sensitivity of the procedure to the ordering.

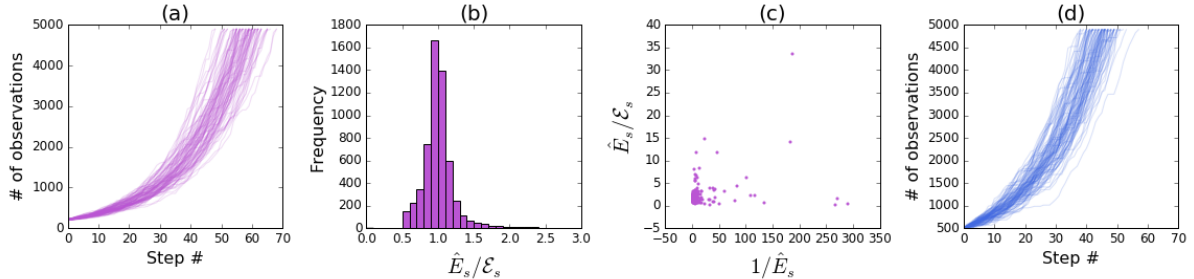


Figure 2: Adaptive path selection for the linear regression model. (a) Distribution of paths chosen by the adaptive approach. (b) Distribution of the estimated L_2 distance relative to the true L_2 distance for transitions with $1/\hat{E}_s \leq 2$. (c) Relative size for steps with bad transitions, i.e. $1/\hat{E}_s \geq 2$. (d) Distribution of paths chosen by the hybrid algorithm

The results of the simulation experiment are displayed in Figure 2. The number of steps required by the adaptive procedure grows logarithmically with the number of observations, providing evidence of the efficiency of the data tempering approach. This advantage comes at a cost; a key difference between tempering and data tempering is that the data tempering approach is more likely to fail at controlling the L_2 distance. This occurs when the next observation in the tempering sequence results in a transition with $\hat{E}_{s,1} \leq \mathcal{E}$ leading to uncontrolled error. Across all experiments, nearly 5% of the steps resulted in no candidate distributions satisfying $\hat{E}_{s,1} \geq \mathcal{E}$; this tends to occur when moving to a high-leverage point, which results in large changes to the posterior. The relative error of these steps is shown in Figure 2(c). These steps are characterized by large L_2 distances, which are often catastrophically underestimated.

This problem occurs because sequential introduction of data points has effectively established an SMC step size that is too large, leading to an insufficiently rich set of possible paths. To address this problem, we present a hybrid path that combines the computational advantages of the data tempering with the rich set of paths afforded by tempering. This hybrid path generally ensures that a satisfactory transition can be made at each step of the algorithm and is specified as follows.

Hybrid path for sequential data: Assume the same setting as the data tempered path and suppose $\mu_{s-1}(x) \propto p(y_{1:k_{s-1}}|x)\pi_0(x)$. First, consider the move to $\nu_{s,1}(x) \propto p(y_{1:k_{s-1}+1}|x) \cdot \pi_0(x)$. If $\hat{E}_{s,1} \geq \mathcal{E}$, consider additional candidate distributions using the data tempering approach. If not, choose candidate distributions in the same manner as the geometric path, selecting from the family $\eta \propto p(y_{1:k_{s-1}} | x)p(y_k | x)^\beta \pi_0(x)$ for $\beta \in [0, 1]$. Several tempering steps may be required to reach $p(y_{1:k_s+1} | x)$, at which time we again consider both data-tempering and tempering moves.

The hybrid path provides a solution to the problem of unacceptably large transitions induced by influential data points. The tempering steps allow for smaller changes in the posterior, effectively allowing for fractional data points in order to refine the step size. Applying the hybrid approach to the Bayesian linear regression example results in the adaptive criteria being satisfied at each step, with no failed tran-

sitions and accurate estimation of the L_2 distances. These paths are shown in Figure 2(d). Somewhat surprisingly, these paths tend to be shorter than those from the data tempered approach. This is due to a cascading effect; following a poor transition there is increased error in the estimation of the L_2 distance, resulting in unnecessarily conservative transitions.

6 Conclusion

The results presented in this paper demonstrate the importance of path selection in the design of SMC sampling algorithms. Proper selection of paths has the potential to dramatically improve the efficiency of SMC; for some target distributions the resulting bounds have lower complexity than those for MCMC. When an efficient path is not known prior to running the algorithm, adequate paths can in some cases be obtained during sampling by adaptively choosing steps using the RESS as an estimate of the L_2 distance. In the examples presented here this leads to near-optimal paths, although we currently have no theoretical guarantees of optimality, only sufficiency. More general approaches to automatic construction of efficient paths may provide further improvements for practical applications.

Appendices

A Proof of Theorem 1

The proof follows closely the approach in [14]. The key is to ensure that after each step of the algorithm the following holds with high probability

$$\begin{aligned} \mathbf{C}_s(\text{i}) \quad & X_s^n \sim \mu_s \text{ for } n = 1, \dots, N \\ \mathbf{C}_s(\text{ii}) \quad & \bar{w}_{s+1} \geq \mu_s(w_{s+1}) \cdot \frac{2}{3} \end{aligned} \tag{9}$$

This is called the one-step induction condition. When $\mathbf{C}_s(\text{i})$ and $\mathbf{C}_s(\text{ii})$ hold, the marginal distribution of the re-sampled particles is 2-warm for μ_{s+1} by Lemma 3 of [14]. Then, using a coupling argument and martingale concentration inequalities, conditions $\mathbf{C}_{s+1}(\text{i})$ and $\mathbf{C}_{s+1}(\text{ii})$ can be shown to hold using Corollary 3.1 and Lemma 4 of [14], respectively. Inductively applying these steps leads to the proof of Theorem 1 in [14].

We modify this proof by showing an alternate condition under which $\mathbf{C}_s(\text{ii})$ holds. This result uses a different kind of martingale concentration and replaces Lemma 4 of [14].

Lemma 3 (Lower bound on the average weights).

Fix any $0 < \delta_0 < 1$ and choose $N \geq 81 \log(2/\delta_0) \cdot \|\mu_s/\mu_{s-1}\|_{L_2(\mu_{s-1})}$. Then, conditional on $\mathbf{C}_{s-1}(i)$,

$$\Pr\left(\bar{w}_s \geq \mu_{s-1}(w_s) \cdot 2/3\right) \geq 1 - \delta_0/2$$

Proof. Let $Y^n = \min\{w_s(X_s^n), \alpha\}$ with $\alpha = \mu_{s-1}(w_s^2)/6\mu_{s-1}(w_s)$ and sample mean \bar{Y} . Define the residual errors to be $\mathcal{Y}^n = \sum_{i=1}^n (Y^i - \mathbf{E}Y^i)$. Using the same approach as in Lemma 4 of [14] we can show that \mathcal{Y}^n is a zero-mean martingale. The martingale has increments bounded by α as $\mathcal{Y}^{n-1} - \mathcal{Y}^n \leq \mathbf{E}Y_n \leq \alpha$. The variance of each increment is bounded as follows:

$$\begin{aligned} \text{Var}(\mathcal{Y}^n | \mathcal{Y}^{n-1}) &= \text{Var}(Y^n - \mathbf{E}Y^n | \mathcal{Y}^{n-1}) \\ &\leq \text{Var}(Y^n - \mathbf{E}Y^n) \\ &\leq \mu_{s-1}(w_s^2) \end{aligned} \tag{10}$$

These conditions verify the requirements of Theorem 22 in [36]. This gives

$$\Pr\left(\mathcal{Y}^N/N \leq -\epsilon\right) \leq \exp\left(\frac{N\epsilon^2}{\mu_{s-1}(w_s^2) \cdot (2 + \epsilon/18\mu_{s-1}(w_s))}\right) \tag{11}$$

Therefore choosing $\epsilon = \mu_{s-1}(w_s)/6$ and $N \geq 81 \log(2/\delta_0)/\mathcal{E}$ ensures $\Pr(\bar{Y} - \mathbf{E}Y_1 \geq -\mu_{s-1}(w_s)/6) \geq 1 - \delta_0/2$. The condition $\bar{Y} - \mathbf{E}Y_1 \geq -\mu_{s-1}(w_s)/6$ is sufficient to show that the claim holds with probability at least $1 - \delta_0$:

$$\begin{aligned} \bar{w}_{s+1} &\geq \bar{Y} \\ &\geq \mathbf{E}Y_1 - \mu_{s-1}(w_s)/6 \\ &\geq \mu_{s-1}(w_s) - \mu_{s-1}(w_s^2)/\alpha - \mu_{s-1}(w_s)/6 \\ &\geq \mu_{s-1}(w_s) \cdot 2/3 \end{aligned} \tag{12}$$

The third line follows from Lemma 3.9 of [15] and the final line follows from the choice of α . ■

This inequality can be used to prove the following one step induction condition, the proof of which is the same as corollary 4.1 of [14]

Corollary 3.1 (One step induction condition).

Assume $P(\mathbf{C}_{s-1}(ii)) \geq 3/4$. Fix $0 < \delta_0 < 1$. Choose $N \geq 81 \log(2/\delta_0) \cdot \|\mu_s/\mu_{s-1}\|_{L_2(\mu_{s-1})}$ and $t \geq \tau_s(\frac{\delta_0}{2N}, 2)$. Then the inductive condition $\mathbf{C}_s|\mathbf{C}_{s-1}$ holds with probability at least $1 - \delta_0$

The proof of Theorem 1 follows immediately as in [14] using the new one step induction condition.

A.1 Gaussian example

First, we derive the L_2 distance from $\eta \sim N(\theta_0, \phi_0^{-1})$ to $\mu \sim N(\theta_1, \phi_1^{-1})$ on \mathcal{R} , assuming $2\phi_1 \geq \phi_0$. We have

$$\|\mu/\eta\|_{L_2(\eta)} = \frac{\phi_1}{\phi_0^{1/2}} \int \frac{1}{\sqrt{2\pi}} \exp(-0.5[2\phi_1(x - \theta_1)^2 - \phi_0(x - \theta_0)^2]) \quad (13)$$

Let $\phi^* = 2\phi_1 - \phi_0$ and $\theta^* = 2\phi_1\theta_1 - \phi_0\theta_0$ and complete the square inside the exponential function.

$$\begin{aligned} 2\phi_1(x - \theta_1)^2 - \phi_0(x - \theta_0)^2 &= \phi^*(x - \theta^*/\phi^*)^2 + 2\phi_1\theta_1^2 - \phi_0\theta_0^2 - \frac{\theta^{*2}}{\phi^*} \\ &= \phi^*(x - \theta^*/\phi^*)^2 - \frac{2\phi_1\phi_0}{\phi^*}(\theta_1 - \theta_0)^2 \end{aligned} \quad (14)$$

Inserting (14) into (13) and substituting $\psi = \phi_1/\phi_0$ gives

$$\|\mu/\eta\|_{L_2(\eta)} = \frac{\psi}{\sqrt{2\psi - 1}} \exp\left(\frac{\phi_1}{2\psi - 1}(\theta_1 - \theta_0)^2\right)$$

The L_2 distance for spherical, d -dimensional Gaussians follows immediately:

$$\|\mu/\eta\|_{L_2(\eta)} = \left(\frac{\psi^2}{2\psi - 1}\right)^{d/2} \exp\left(\frac{d\phi_1}{2\psi - 1}(\theta_1 - \theta_0)^2\right) \quad (15)$$

A.2 Geometric path

The geometric path from section 3.1 consists of a sequence of Gaussian distributions with $\mu_{\beta_s}(x) = N(\mathbf{1}_d \cdot \theta_s, I_d/\phi_s)$ where $\theta_s = \theta \cdot \beta_s/\phi_s$ and $\phi_s = \beta_s(\phi - 1) + 1$. We remind the reader that $\phi > 1$ and $\theta \geq 2$ and proceed to bound the L_2 distance by separately bounding the factors in (15). Define $\psi_s = \phi_s/\phi_{s-1}$. For $s = 1:d$

$$\begin{aligned} 1 < \psi_1 &= 1 + \frac{\phi - 1}{\phi \cdot \theta \sqrt{d}} \\ &\leq 1 + \frac{2}{\theta \sqrt{d}} \end{aligned} \quad (16)$$

and when $s > 1$:

$$\begin{aligned} 1 \leq \psi_s &= \frac{\beta_s(\phi - 1) + 1}{\beta_{s-1}(\phi - 1) + 1} \\ &= 1 + \frac{(\beta_s - \beta_{s-1})(\phi - 1)}{\beta_{s-1}(\phi - 1) + 1} \\ &\leq 1 + \frac{(\beta_s - \beta_{s-1})}{\beta_{s-1}} \\ &= 1 + \frac{2}{\theta \sqrt{d}} \end{aligned} \quad (17)$$

Plugging this into the factor $\left(\frac{\psi^2}{2\psi-1}\right)^{d/2}$ in the L_2 distance (15) gives

$$\begin{aligned} \left(\frac{\psi_s^2}{2\psi_s-1}\right)^{d/2} &\leq \left(\frac{\left(1+\frac{2}{\theta\sqrt{d}}\right)^2}{\left(1+\frac{4}{\theta\sqrt{d}}\right)}\right)^{d/2} \\ &\leq \left(1+\frac{1}{d}\right)^{d/2} \\ &\leq 2 \end{aligned} \tag{18}$$

where the second line uses $\theta \geq 2$. To bound the second factor in (15) we bound the difference in means. For $s = 1$, $\theta_1 - \theta_0 = \frac{1}{\phi\sqrt{d}\cdot\phi_1} \leq \frac{1}{\sqrt{d}\phi_1}$ and consequently $\exp\left(\frac{d\phi_1}{2\psi_1-1}(\theta_1 - \theta_0)^2\right) \leq e$. For $s > 1$:

$$\begin{aligned} \theta_s - \theta_{s-1} &= \theta\left(\frac{\beta_s}{\phi_s} - \frac{\beta_{s-1}}{\phi_{s-1}}\right) \\ &= \frac{\theta \cdot \beta_{s-1}}{\phi_{s-1}\phi_s} \left(\left(1 + \frac{2}{\theta\sqrt{d}}\right)\phi_{s-1} - \phi_s\right) \\ &= \frac{2\beta_{s-1}}{\phi_{s-1}\phi_s\sqrt{d}} \end{aligned} \tag{19}$$

Inserting this result into the second term in (15) gives

$$\begin{aligned} \exp\left(\frac{d\phi_1}{2\psi-1}(\theta_1 - \theta_0)^2\right) &= \exp\left(\frac{4\beta_{s-1}^2}{2\phi_s^2\phi_{s-1} - \phi_s\phi_{s-1}^2}\right) \\ &\leq \exp(4) \end{aligned} \tag{20}$$

The first line follows using $1 \leq \phi_{s-1} \leq \phi_s$ and $\beta_s \leq 1$. Inserting (18) and (19) into (15) shows that for the geometric path $1/\mathcal{E} = \mathcal{O}(1)$ proving (4).

A.3 Precision path

The precision path is specified by a sequence of normal distributions $\mu_s = N_d(\theta_s, I_d/\phi_s)$. The location parameter is $\theta_s = 0$ for $s \leq s_1 = \lceil 3\sqrt{d} \log(d\theta^2) \rceil$ and $\theta_s = 1_d\theta$ otherwise. The precisions are given by

$$\phi_s = \begin{cases} \left(1 - \frac{1}{\sqrt{9d}}\right)^s \vee \frac{1}{d\theta^2}, & \text{if } 0 \leq s \leq s_1 \\ \frac{1}{d\theta^2} \left(1 + \frac{1}{\sqrt{d}}\right)^{s-s_1-1} \wedge \phi, & \text{otherwise} \end{cases} \tag{21}$$

Let $\psi_s = \phi_s/\phi_{s-1}$. When $s \leq s_1$, $1 \geq \psi_s \geq \left(1 - \frac{1}{\sqrt{9d}}\right)$ and therefore

$$\begin{aligned} \|\mu_s\|_{L_2(\mu_{s-1})} &= \left(\frac{\psi_s^2}{2\psi_s-1}\right)^{d/2} \\ &\leq \left(\frac{\left(1 - \frac{1}{\sqrt{9d}}\right)^2}{\left(1 - \frac{2}{\sqrt{9d}}\right)}\right)^{d/2} \\ &\leq \left(1 + \frac{1}{d}\right)^{d/2} \\ &\leq 2 \end{aligned} \tag{22}$$

The same approach shows that $\|\mu_s/\mu_{s-1}\|_{L_2(\mu_{s-1})} \leq 2$ for $s \geq s_1 + 2$. When $s = s_1 + 1$, $\phi_s = 1$ and therefore $\|\mu_s/\mu_{s-1}\|_{L_2(\mu_{s-1})} = 1$. therefore $1/\mathcal{E} \leq 2$, proving (5).

B Proof of Theorem 2

The proof of Theorem 2 follows in a similar manner to Theorem 1. To incorporate the adaptive selection of distributions, we add the following condition in addition to those in (9)

$$\mathbf{C}_s(\text{iii}) \quad \|\mu_{s+1,n}/\mu_s\|_{L_2(\mu_s)} \leq 3/\hat{E}_{s+1,m} \quad (23)$$

This condition will be used to ensure that, for any adaptively chosen distribution $\mu_s = \nu_{s,m}$, that $\mathbf{C}_s(\text{ii})$ holds with high probability using Lemma (3). This allows the construction of an adaptive version of the one step induction condition, which will then be used to prove Theorem 2. Before proving the inductive condition, we give conditions under which $\mathbf{C}_s(\text{iii})$ holds for any $\nu_{s,m}$ with high-probability.

Lemma 4 (Adaptive selection of distributions).

Suppose at the beginning of step s we have m candidate distributions $\nu_{s,1}, \dots, \nu_{s,M}$ and that condition $\mathbf{C}_{s-1}(i)$ holds. Let $w_{s,m} \propto \nu_{s,m}(x)$ and assume that $0 < w_{s,m} \leq 1$ for each m and let $\bar{w}_{s,m}^2 = \frac{1}{N} \sum_{n=1}^N w_{s,m}(X_{s-1}^n)^2$. Choose any $0 < C < 1$ and $0 < \delta_0 < 1$. Then for $N \geq \frac{32}{C^2} \cdot \log\left(\frac{12M}{\delta_0}\right)$ and every m s.t. $\bar{w}_{s,m}^2 \geq C$:

$$\Pr\left(\|\nu_{s,m}/\mu_{s-1}\|_{L_2(\mu_{s-1})} \leq 3/\hat{E}_{s,m}\right) \geq 1 - \delta_0/3$$

Proof. Azuma's inequality ensures that for this choice of N and any $f \in \mathcal{F}$ with $|f| \leq 1$ that $\Pr(|\bar{f} - \mu_{s-1}f| \geq C/4) \leq \delta_0/6M$. Applying a union bound gives the following

$$\begin{aligned} & \Pr\left(\bigcup_{m=1}^M \{|\bar{w}_{s,m} - \mu_{s-1}(w_{s,m})| \geq C/4\} \cup \{|\bar{w}_{s,m}^2 - \mu_{s-1}(w_{s,m}^2)| \geq C/4\}\right) \\ & \leq \max_m \Pr\left(|\bar{w}_{s,m} - \mu_{s-1}(w_{s,m})| \geq C/4\right) \vee \Pr\left(|\bar{w}_{s,m}^2 - \mu_{s-1}(w_{s,m}^2)| \geq C/4\right) \\ & \leq \delta_0/3 \end{aligned} \quad (24)$$

Now we show that if $\bar{w}_{s,m}^2 \geq C$ that it estimates $\mu_{s-1}(w_{s,m}^2)$ with small relative error. Assume that $|\bar{w}_{s,m}^2 - \mu_{s-1}(w_{s,m}^2)| \leq C/4$. Then $\mu_{s-1}(w_{s,m}^2) \geq \bar{w}_{s,m}^2 - C/4 \geq C \cdot 3/4$ and therefore

$$|\bar{w}_{s,m}^2 - \mu_{s-1}(w_{s,m}^2)| \leq C/4 \leq \mu_{s-1}(w_{s,m}^2)/3 \quad (25)$$

A similar argument gives $|\bar{w}_{s,m} - \mu_{s-1}(w_{s,m})| \leq \mu_{s-1}(w_{s,m})/3$, noticing that $C \leq \bar{w}_{s,m}^2 \leq \bar{w}_{s,m}$ as $0 < w_{s,m} < 1$. This shows that

$$\frac{1}{\hat{E}_{s,m}} \geq \frac{3\mu_{s-1}(w_{s,m}^2)}{8(\mu_{s-1}(w_{s,m}))^2} \geq \frac{1}{3} \|\nu_{s,m}/\mu_{s-1}\|_{L_2(\mu_{s-1})} \quad (26)$$

Combining (24) and (26) gives the result. ■

The adaptive one step induction condition follows from combining Lemma 4 with Corollary 3.1.

Lemma 5 (Adaptive one step induction condition).

Suppose at the beginning of step s we have M candidate distributions $\nu_{s,1}, \dots, \nu_{s,M}$ with $0 < w_{s,m} \leq 1$ and that condition $\mathbf{C}_{s-1}(i)$ holds. Fix a lower bound $0 < C < 1$, a target effective sample size $0 < \mathcal{E} < 1$, and a probability $0 < \delta_0 < 1$. Choose:

$$\mu_s = \max_m \left\{ \nu_{s,m} : \frac{1}{\hat{E}_{s,m}} \leq \frac{1}{\mathcal{E}} \text{ and } \bar{w}_{s,m}^2 \geq C \right\} \quad (27)$$

Then for $N \geq \frac{32}{C^2} \cdot \log\left(\frac{12M}{\delta_0}\right) \vee \frac{243}{\mathcal{E}} \cdot \log\left(\frac{3}{\delta_0}\right)$ and $t \geq \tau_{s+1}\left(\frac{\delta_0}{3N}, 2\right)$

$$\Pr\left(\mathbf{C}_s(i) \mid \mathbf{C}_{s-1}(i)\right) \geq 1 - \delta_0$$

Proof. For this choice of μ_s it follows from Lemma 4 that:

$$\Pr(\mathbf{C}_s(\text{iii}) \mid \mathbf{C}_{s-1}(\text{i})) \geq 1 - \delta_0/3$$

This allows us to apply Corollary 3.1 with $\|\mu_s/\mu_{s-1}\|_{L_2(\mu_{s-1})} \leq 3/\mathcal{E}$.

$$\begin{aligned} \Pr(\mathbf{C}_s(\text{i}) \mid \mathbf{C}_{s-1}(\text{i})) &\geq \Pr(\mathbf{C}_s(\text{i}) \cap \mathbf{C}_{s-1}(\text{ii}) \cap \mathbf{C}_{s-1}(\text{iii}) \mid \mathbf{C}_{s-1}(\text{i})) \\ &\geq \Pr(\mathbf{C}_s(\text{i}) \cap \mathbf{C}_{s-1}(\text{ii}) \mid \mathbf{C}_{s-1}(\text{iii}), \mathbf{C}_{s-1}(\text{i})) \\ &\quad \cdot \Pr(\mathbf{C}_{s-1}(\text{iii}) \mid \mathbf{C}_{s-1}(\text{i})) \\ &\geq 1 - \delta_0 \end{aligned} \tag{28}$$

■

The proof of Theorem 2 follows by combining Theorem 1 and Corollary 5.

Proof of Theorem 2

Proof. Let $\delta_p = \frac{1}{8} \sum_{i=0}^{p-1} 2^{-i} < \frac{1}{4}$ and define the inductive epoch condition:

$$\Pr(\mathbf{C}_{Sp}) \geq 1 - \delta_p \tag{29}$$

This condition will ensure that the result holds for any $s \leq Sp$. To show this holds for $p = 1$, use the same approach as in Theorem 1, replacing Corollary 3.1 with Corollary 5. We now prove that the inductive step holds.

Suppose that at the end of epoch $p - 1$ we have not reached the target distribution and that (29) holds. First, we show that condition $\tilde{\mathbf{C}}_{S(p-1)}$ holds for the new particle approximation with probability at least $1 - \frac{1}{8}2^{-p}$ for the specified N_p and t_p . The tilde notation is used to distinguish between the induction conditions for the current particle system and the new particle system. This follows from Theorem 1 conditional on (29), suitably modified for this probability, noting that (29) ensures $\max_{s=1, \dots, S(p-1)} \|\mu_s/\mu_{s-1}\|_{L_2(\mu_{s-1})} \leq 3/\mathcal{E}$. Therefore

$$\begin{aligned} \Pr(\tilde{\mathbf{C}}_{S(p-1)} \cap \mathbf{C}_{S(p-1)}) &= \Pr(\tilde{\mathbf{C}}_{S(p-1)} \mid \mathbf{C}_{S(p-1)}) \Pr(\mathbf{C}_{S(p-1)}) \\ &\geq 1 - \delta_{p-1} - \frac{1}{8}2^{-p} \end{aligned} \tag{30}$$

As a consequence, the combined particle system also satisfies the induction condition. The next step is to show that the combined particle approximation with $N = \sum_{i=1}^p N_i$ particles using $t = t_p$ Markov kernel transitions ensures the stability of the adaptive approach for next S steps. The chosen values ensure that Corollary 5 holds with $\delta_0 = \frac{1}{8}2^{-p}/S$. Then for s in $S(p-1) + 1, \dots, Sp$:

$$\begin{aligned} \Pr(\mathbf{C}_s) &\geq \prod_{r=S(p-1)+1}^s \Pr(\mathbf{C}_r \mid \mathbf{C}_r) \cdot \Pr(\mathbf{C}_{S(p-1)+1} \mid \tilde{\mathbf{C}}_{S(p-1)} \cup \mathbf{C}_{S(p-1)}) \cdot \Pr(\tilde{\mathbf{C}}_{S(p-1)} \cap \mathbf{C}_{S(p-1)}) \\ &\geq (1 - \frac{1}{8}2^{-p}/S)^s \cdot (1 - \delta_{p-1} - \frac{1}{8}2^{-p}) \\ &\geq 1 - \delta_p \end{aligned} \tag{31}$$

This verifies that (29) holds for epoch p , completing the inductive proof. If the algorithm terminates during epoch p , conditional on the induction condition, the chosen $N = \sum_{i=1}^p N_i$ and t_p ensure that the result holds (see [14] Theorem 1 for additional details). ■

C Bayesian linear regression example

The specified Bayesian linear model leads to a Normal Inverse-Gamma posterior distribution with $\mu_s(\beta, \sigma^2 \mid X_{1:k_s}, Y_{1:k_s}) = \mathcal{N}(\beta \mid \theta_s, \sigma_s^2 \Sigma_s) \cdot \text{Inv-Gamma}(\sigma^2 \mid a_s, b_s)$ where

$$\begin{aligned}\Sigma_s &= (\Sigma_0 + X_{1:k_s}^T X_{1:k_s})^{-1} \\ \theta_s &= \Sigma_s X_{1:k_s}^T Y_{1:k_s} \\ a_s &= 4 + k_s/2 \\ b_s &= 4 + \frac{1}{2}(Y_{1:k_s}^T Y_{1:k_s} - \theta_s^T \Sigma_s^{-1} \theta_s)\end{aligned}\tag{32}$$

and $\Sigma_0 = (X_{1:K}^T X_{1:K})^{-1}/K$. The L_2 distance is:

$$\|\mu_s/\mu_{s-1}\|_{L_2(\mu_{s-1})} = \int \frac{\mathcal{N}^2(\beta \mid \theta_{s-1}, \sigma^2 \Sigma_{s-1}) \cdot \text{Inv-gamma}^2(\sigma^2 \mid a_{s-1}, b_{s-1})}{\mathcal{N}(\beta \mid \theta_s, \sigma^2 \Sigma_s) \cdot \text{Inv-gamma}(\sigma^2 \mid a_s, b_s)} d\beta d\sigma^2\tag{33}$$

The conditional normal distribution on β can be integrated out by completing the square:

$$\begin{aligned}\int \frac{\mathcal{N}^2(\beta \mid \theta_{s-1}, \sigma^2 \Sigma_{s-1})}{\mathcal{N}(\beta \mid \theta_s, \sigma^2 \Sigma_s)} d\beta &= \int \frac{|2\pi\sigma^2 \Sigma_{s-1}|^{-1} \exp\left(-\frac{1}{\sigma^2}(\beta - \theta_{s-1})^T \Sigma_{s-1}^{-1}(\beta - \theta_{s-1})\right)}{|2\pi\sigma^2 \Sigma_s|^{-1/2} \exp\left(-\frac{1}{2\sigma^2}(\beta - \theta_s)^T \Sigma_s^{-1}(\beta - \theta_s)\right)} d\beta \\ &= \frac{|\Sigma_s|^{1/2} |\Sigma_*|^{1/2}}{|\Sigma_{s-1}|} \exp\left(-\frac{b_*}{\sigma^2}\right)\end{aligned}\tag{34}$$

where $\Sigma_* = (2\Sigma_{s-1}^{-1} - \Sigma_s^{-1})^{-1}$, $\mu_* = \Sigma_* (2\Sigma_{s-1}^{-1} \theta_{s-1} - \Sigma_s^{-1} \theta_s)$, and $b_* = \frac{1}{2}[2\theta_{s-1}^T \Sigma_{s-1}^{-1} \theta_{s-1} - \theta_s^T \Sigma_s^{-1} \theta_s - \theta_*^T \Sigma_*^{-1} \theta_*]$. The L_2 distance can be found by integrating the resulting unnormalized gamma pdf:

$$\begin{aligned}\|\mu_s/\mu_{s-1}\|_{L_2(\mu_{s-1})} &= \int \frac{\text{Inv-gamma}^2(\sigma^2 \mid a_{s-1}, b_{s-1})}{\text{Inv-gamma}(\sigma^2 \mid a_s, b_s)} \cdot \frac{|\Sigma_s|^{1/2} |\Sigma_*|^{1/2}}{|\Sigma_{s-1}|} \exp\left(-\frac{b_*}{\sigma^2}\right) d\sigma^2 \\ &= \frac{|\Sigma_s|^{1/2} |\Sigma_*|^{1/2}}{|\Sigma_{s-1}|} \cdot \frac{b_{s-1}^{2a_{s-1}}}{b_s^{a_s} (b_* + 2b_{s-1} - b_s)^{2a_{s-1} - a_s}} \cdot \frac{\Gamma(a_s) \Gamma(2a_{s-1} - a_s)}{\Gamma(a_{s-1})^2}\end{aligned}\tag{35}$$

References

- [1] Andrew Gelman and Xiao-Li Meng. Simulating normalizing constants: from importance sampling to bridge sampling to path sampling. *Statist. Sci.*, 13(2):163–185, 05 1998.
- [2] Ming Lin, Rong Chen, and Jun S. Liu. Lookahead strategies for sequential Monte Carlo. *Statist. Sci.*, 28(1):69–94, 02 2013.
- [3] Nicolas Chopin. A sequential particle filter method for static models. *Biometrika*, 89(3):539–552, 2002.
- [4] Pierre Del Moral, Arnaud Doucet, and Ajay Jasra. Sequential Monte Carlo samplers. *Journal of the Royal Statistical Society: Series B (Statistical Methodology)*, 68(3):411–436, 2006.
- [5] Radford M. Neal. Annealed importance sampling. *Statistics and Computing*, 11(2):125–139, 2001.
- [6] Yan Zhou, Adam M. Johansen, and John A.D. Aston. Toward automatic model comparison: an adaptive sequential Monte Carlo approach. *Journal of Computational and Graphical Statistics*, 25(3):701–726, 2016.

- [7] Ajay Jasra, David A. Stephens, Arnaud Doucet, and Theodoros Tsagaris. Inference for Lévy-driven stochastic volatility models via adaptive sequential Monte Carlo. *Scandinavian Journal of Statistics*, 38(1):1–22, 2011.
- [8] Nick Whiteley. Sequential Monte Carlo samplers: error bounds and insensitivity to initial conditions. *Stochastic Analysis and Applications*, 30(5):774–798, 2012.
- [9] Nikolaus Schweizer. *Non-asymptotic error bounds for sequential MCMC methods*. PhD thesis, University of Bonn, 2011.
- [10] Ajay Jasra, Daniel Paulin, and Alexandre H. Thiery. Error bounds for sequential Monte Carlo samplers for multimodal distributions. *arXiv preprint arXiv:1509.08775*, 2015.
- [11] Nicolas Chopin. Central limit theorem for sequential Monte Carlo methods and its application to Bayesian inference. *The Annals of Statistics*, 32(6):2385–2411, 2004.
- [12] Randal Douc and Eric Moulines. Limit theorems for weighted samples with applications to sequential Monte Carlo methods. *Ann. Statist.*, 36(5):2344–2376, 10 2008.
- [13] Pierre Del Moral. *Feynman-Kac Formulae: Genealogical and Interacting Particle Systems with Applications*. Springer-Verlag, 2004.
- [14] Joe Marion and Scott C. Schmidler. Finite sample complexity of sequential Monte Carlo estimators. *ArXiv e-prints, in preparation*, March 2018.
- [15] László Lovász and Santosh Vempala. Fast algorithms for logconcave functions: sampling, rounding, integration and optimization. In *2006 47th Annual IEEE Symposium on Foundations of Computer Science (FOCS'06)*, pages 57–68, Oct 2006.
- [16] Raaz Dwivedi, Yuansi Chen, Martin J. Wainwright, and Bin Yu. Log-concave sampling: Metropolis-Hastings algorithms are fast! *arXiv preprint arXiv:1509.08775*, 01 2018.
- [17] László Lovász and Santosh Vempala. Hit-and-run from a corner. In *Proceedings of the Thirty-sixth Annual ACM Symposium on Theory of Computing*, STOC '04, pages 310–314, New York, NY, USA, 2004. ACM.
- [18] Santosh Vempala. Geometric random walks: a survey. *Combinatorial and Computational Geometry*, pages 573–612, 2005.
- [19] Rajeev Motwani and Prabhakar Raghavan. *Randomized Algorithms*. Cambridge University Press, New York, NY, USA, 1995.
- [20] Mark R. Jerrum, Leslie G. Valiant, and Vijay V. Vazirani. Random generation of combinatorial structures from a uniform distribution. *Theoretical Computer Science*, 43:169 – 188, 1986.
- [21] Gareth Roberts, Jeffrey Rosenthal, et al. Geometric ergodicity and hybrid Markov chains. *Electronic Communications in Probability*, 2:13–25, 1997.
- [22] Gareth O. Roberts and Richard L. Tweedie. Geometric L^2 and L^1 convergence are equivalent for reversible Markov Chains. *Journal of Applied Probability*, 38:37–41, 2001.
- [23] Nial Friel, Merrilee Hurn, and Jason Wyse. Improving power posterior estimation of statistical evidence. *Statistics and Computing*, 24(5):709–723, Sep 2014.

- [24] Gareth O. Roberts and Richard L. Tweedie. Exponential convergence of Langevin distributions and their discrete approximations. *Bernoulli*, 2(4):341–363, 12 1996.
- [25] László Lovász and Santosh Vempala. The geometry of logconcave functions and sampling algorithms. *Random Structures & Algorithms*, 30(3):307–358, 2006.
- [26] László Lovász and Santosh Vempala. Simulated annealing in convex bodies and an $\mathcal{O}^*(n^4)$ volume algorithm. *Journal of Computer and System Sciences*, 72(2):392 – 417, 2006. JCSS FOCS 2003 Special Issue.
- [27] Garland Durham and John Geweke. *Adaptive sequential posterior simulators for massively parallel computing environments*, chapter 1, pages 1–44. Emerald Group Publishing Limited, 2014.
- [28] Luca Martino, Victor Elvira, and Francisco Louzada. Alternative effective sample size measures for importance sampling. In *2016 IEEE Statistical Signal Processing Workshop (SSP)*, pages 1–5, June 2016.
- [29] Thi Le Thu Nguyen, Francois Septier, Gareth W. Peters, and Yves Delignon. Efficient sequential Monte Carlo samplers for Bayesian inference. *IEEE Transactions on Signal Processing*, 64(5):1305–1319, March 2016.
- [30] Ruslan Salakhutdinov. Learning and evaluating Boltzmann machines. Technical report, University of Toronto, 2008.
- [31] Sudipto Bannerjee, Bradley P. Carlin, and Alan E. Gelfand. *Hierarchical Modeling and Analysis for Spatial Data, Second Edition*. Chapman and Hall/CRC, 2014.
- [32] D. W. K. Binder, Heermann. *Monte Carlo Simulation in Statistical Physics: an Introduction*. Springer, 2002.
- [33] James Gary Propp and David Bruce Wilson. Exact sampling with coupled Markov Chains and applications to statistical mechanics. *Random Struct. Algorithms*, 9(1-2):223–252, August 1996.
- [34] Dawn B. Woodard, Scott C. Schmidler, and Mark Huber. Conditions for rapid mixing of parallel and simulated tempering on multimodal distributions. *Annals of Applied Probability*, pages 617–640, 2009.
- [35] Dua Dheeru and Efi Karra Taniskidou. UCI machine learning repository, 2017.
- [36] Fan Chung and Linyuan Lu. Concentration inequalities and martingale inequalities: a survey. *Internet Math.*, 3(1):79–127, 2006.